JOURNAL OF CATALYSIS 101, 114–122 (1986)

Role of NO in Inhibiting CO Oxidation over Alumina-Supported Rhodium

SE H. OH AND JOYCE E. CARPENTER[1]

Physical Chemistry Department, General Motors Research Laboratories, Warren, Michigan 48090-9055

Received January 21, 1986; revised April 18, 1986

The inherent rate of the $CO-O_2$ reaction over alumina-supported Rh is much higher than that of the CO–NO reaction. Rate measurements in $CO-NO-O_2$ mixtures have shown, however, that the presence of even small amounts of NO in the reactant stream prevents the occurrence of the $CO-O_2$ reaction until the extent of the CO–NO reaction becomes significant, resulting in the simultaneous onset of both the $CO-O_2$ and CO–NO reactions near the lightoff temperature for the CO–NO reaction itself (i.e., in the absence of O_2). This indicates that the overall kinetic behavior of Rh/Al_2O_3 in $CO-NO-O_2$ mixtures is dominated by the features characteristic of the CO–NO reaction rather than by those of the $CO-O_2$ reaction. These kinetic interactions among the reactant species, including the NO inhibition effect on the CO oxidation rate, can be interpreted on the basis of a mechanism involving the blocking of the reactive sites by molecularly adsorbed NO. Similar experiments with a Pt/Al_2O_3 catalyst have shown that its CO oxidation activity is much less affected by the presence of NO than is the CO oxidation rate over Rh/Al_2O_3.

INTRODUCTION

The reactions of CO with O_2 and NO over supported noble metal catalysts are important parts of the catalytic control of automobile exhaust emissions (*1–4*). Partly because of their importance in automobile exhaust catalysis, the kinetics and mechanism of the $CO-O_2$ reaction (e.g., Refs. (*5–7*) and the CO–NO reaction (e.g., Refs. (*7–10*) have received considerable attention in the literature of the past decade. Much of the earlier work in this area focused on the single-reaction cases, where each reaction was studied separately. In reality, of course, these two reactions occur simultaneously in a feedstream containing all the reactant species. Thus, it is of considerable practical as well as scientific importance to understand the kinetic features of each of these reactions in $CO-NO-O_2$ mixtures.

One interesting mode of kinetic interaction among the reactant species is the strong inhibition effect of NO on the rate of the $CO-O_2$ reaction. In a kinetic study with a Pt/Al_2O_3 catalyst, Voltz *et al.* (*11*) have observed that the rate of CO oxidation is significantly retarded in the presence of NO in the feedstream. Their rate data can be well described by a kinetic model that assumes the blocking of catalytically active sites by nonreacting NO. Such NO inhibition effects do not appear to be limited to supported Pt catalysts; as this paper will show, a Rh/Al_2O_3 catalyst exhibits an even stronger inhibition of the $CO-O_2$ reaction by NO. The present investigation was undertaken to gain understanding of the kinetic behavior of Rh/Al_2O_3 when CO reacts with a mixture of O_2 and NO. The results of kinetic experiments in $CO-NO-O_2$ mixtures are compared and contrasted with those for the single-reaction cases. Such comparison would allow us to ascertain the nature and extent of kinetic interactions among the reactant species in the three-component feedstream. Of particular interest is the role of NO in inhibiting the CO oxidation rate and in determining the overall kinetics of the $CO-NO-O_2$ reaction system.

EXPERIMENTAL

The experimental apparatus and proce-

[1] Present address: AC Spark Plug Division, General Motors Corp., Flint, Michigan 48556.

0021-9517/86 $3.00

dures used in this study are identical to those described previously (*7, 12*). Steady-state reaction rates were measured using an internal-recycle mixed flow reactor (*13*) equipped with continuous gas analyzers (nondispersive IR for CO and CO_2, polarographic detection for O_2, chemiluminescence detection for NO). A magnetically driven impeller (1500 rpm) provides good gas-phase mixing within the reactor, thus allowing the reactor to be characterized as a CSTR. The reactor operated at atmospheric total pressure and the desired concentrations of the individual reactants were obtained by blending appropriate amounts of the gases in a N_2 background.

Rate data reported here were obtained with the same Rh catalyst (0.01 wt% Rh/Al_2O_3 prepared by the incipient wetness technique with an aqueous solution of $RhCl_3 \cdot 3H_2O$) that was used in our earlier studies (*7, 12*). For comparison purposes, a 0.05 wt% Pt/Al_2O_3 catalyst was also used for some kinetic experiments. This catalyst was prepared by impregnating Grace low-density θ-alumina beads (3.5 mm diameter, 116 m^2/g BET surface area) using a non-aqueous method developed by D'Aniello (*14*). The metal adsorbate solution was obtained by dissolving $H_2PtCl_6 \cdot 6H_2O$ in acetone. After impregnation the catalyst was dried in air overnight at room temperature and then calcined in air at 500°C for 4 h. Such procedures resulted in a shallow Pt band (~30 μm) at the periphery of the catalyst beads.

RESULTS

Before discussing the results of kinetic experiments in CO–NO–O_2 mixtures, it is useful to examine the stoichiometry of the individual reactions over the Rh/Al_2O_3 catalyst. The CO–NO reaction stoichiometry was investigated by conducting a temperature run-up experiment in a feedstream of fixed composition (0.25 vol% CO–0.25 vol% NO in a N_2 background). In this experiment, steady-state outlet concentrations of the reactants (CO and NO) and the product (CO_2) were monitored as a function of temperature. The results obtained over the temperature range of 300 to 400°C are shown in Fig. 1, where the amounts of NO consumption and CO_2 production (ΔNO and ΔCO_2) are plotted against the amount of CO consumed (ΔCO) during the reaction. It can be seen in Fig. 1 that the actual data points lie close to the diagonal lines over the wide range of reactant conversions. This indicates that under steady-state conditions the CO–NO reaction over Rh/Al_2O_3 proceeds such that $\Delta CO \simeq \Delta NO \simeq \Delta CO_2$. It follows directly from these observations and material balance considerations that N_2 is the only major nitrogen-containing reaction product under the conditions of our experiments and thus the reaction stoichiometry can be expressed as

$$CO + NO \rightarrow CO_2 + \tfrac{1}{2} N_2 \qquad (1)$$

Similar experiments under net-reducing feedstream conditions (0.5 vol% CO–0.1 vol% NO) yielded the same stoichiometric equation given above. It was also found that the CO–O_2 reaction over Rh/Al_2O_3 follows the well-established stoichiometric

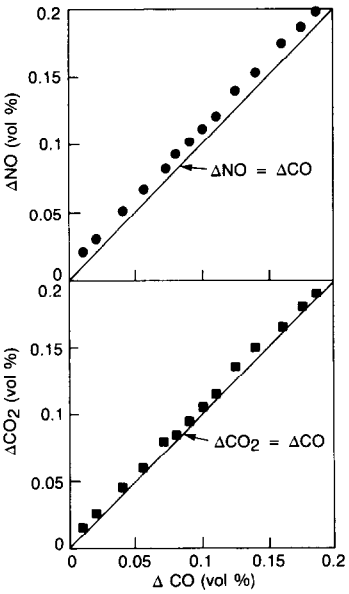

FIG. 1. The CO–NO reaction stoichiometry over 0.01 wt% Rh/Al_2O_3 for a feedstream containing 0.25 vol% CO and 0.25 vol% NO.

equation

$$CO + \tfrac{1}{2} O_2 \rightarrow CO_2 \qquad (2)$$

The CO–NO reaction stoichiometry described by Eq. (1) is in contrast to the observation of Hecker and Bell (*9*) that a relatively large amount of N_2O is formed during NO reduction by CO over a silica-supported Rh catalyst. Although factors affecting the relative amounts of N_2 and N_2O formation are not yet well understood, it is reasonable to speculate that the differences in the nature of the support (Al_2O_3 vs SiO_2), Rh loading (0.01 wt% vs 4.6 wt%), and reaction conditions (generally lower temperatures in the earlier study) might have contributed to the different selectivities observed in these two studies.

We first conducted rate measurements for the CO–O_2 and CO–NO reactions separately in order to compare the reactivity of O_2 and NO toward CO. The results of such experiments are presented in Arrhenius plots of the reaction rates shown by the solid lines in Fig. 2. It is evident that for the same partial pressures of O_2 and NO (0.5 vol% each), the CO–O_2 reaction has a much higher rate than the CO–NO reaction; the temperature required for the onset of the latter reaction is about 80°C higher than that for the former. Our previous kinetic study with the same Rh/Al_2O_3 catalyst

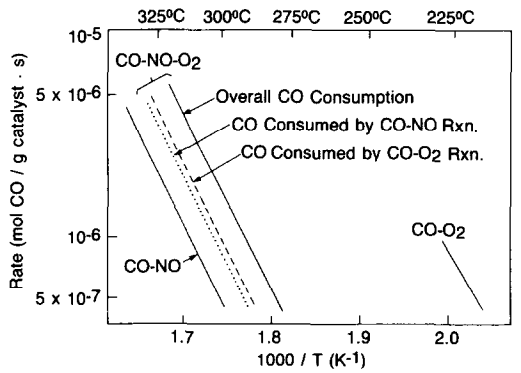

FIG. 2. Arrhenius plots for CO consumption rates over Rh/Al_2O_3 in CO–NO, CO–O_2, and CO–NO–O_2 mixtures. The concentrations of each of the reactants was 0.5 vol% in all cases.

(*7*) indicates that this low reactivity of NO toward CO is related to a slow NO dissociation rate over supported Rh. The observed apparent activation energy of ~46 kcal/mol for the CO–NO reaction can also be rationalized on the basis of a reaction mechanism where the dissociation of molecularly adsorbed NO is the rate-limiting step and both CO and NO are in adsorption equilibrium. The apparent activation energy for the CO–O_2 reaction (~28 kcal/mol) is similar to the activation energy for CO desorption from CO-saturated Rh surfaces (*7*). This is expected because under the conditions of the CO–O_2 reaction, the surface is predominantly covered with adsorbed CO and thus the oxygen adsorption (which is the rate-limiting step) occurs on Rh sites vacated primarily by CO desorption (*5*, *7*).

Also shown in Fig. 2 is the overall reaction rate (i.e., the total amount of CO consumed per unit time per unit mass of catalyst) measured in a reactant gas mixture containing 0.5 vol% CO, 0.5 vol% NO, and 0.5 vol% O_2 in a N_2 background. It is interesting to note that the overall reaction rate in the CO–NO–O_2 mixture lies much closer to the curve for the CO–NO reaction than to the curve for the CO–O_2 reaction. Furthermore, the apparent activation energy for the CO–NO–O_2 reaction system (~42 kcal/mol) is similar to that for the CO–NO reaction (~46 kcal/mol). These observations indicate that the kinetic behavior of the CO–NO–O_2 system is dominated by the CO–NO reaction kinetics rather than by the CO–O_2 reaction kinetics. This is contrary to our expectation that the overall reaction kinetics of parallel reaction systems would be dominated by the reaction that has a faster rate (the CO–O_2 reaction in our case). Similar observations have been made in our laboratory for some CO–HC–O_2 reaction systems catalyzed by noble metals; for example, the oxidation kinetics of olefin hydrocarbons are found to be controlled by the oxidation of CO which has a lower inherent reaction rate.

It is instructive to examine how the rates

of the individual reactions in the CO–NO–O_2 mixture compare with those for the single-reaction cases. The extent of the CO–O_2 and CO–NO reactions in the CO–NO–O_2 mixture (shown by the dotted and dashed lines in Fig. 2) was obtained from measured values of ΔCO, ΔCO_2, and ΔNO based on the reaction stoichiometries given by Eqs. (1) and (2). It can be seen that the rate of the CO–O_2 reaction is strongly suppressed when NO is present in the reacting gas, whereas the CO–NO reaction rate is only mildly affected by the presence of oxygen. Of particular interest is the observation that the NO in the reactant stream prevents the occurrence of the CO–O_2 reaction until the extent of the CO–NO reaction becomes significant, greatly decreasing the activity difference between the two reactions. This strongly suggests that the onset of these two reactions in CO–NO–O_2 mixtures is controlled by the same mechanistic step, as will be discussed below.

Additional kinetic experiments under isothermal conditions (230°C; see Fig. 3) show

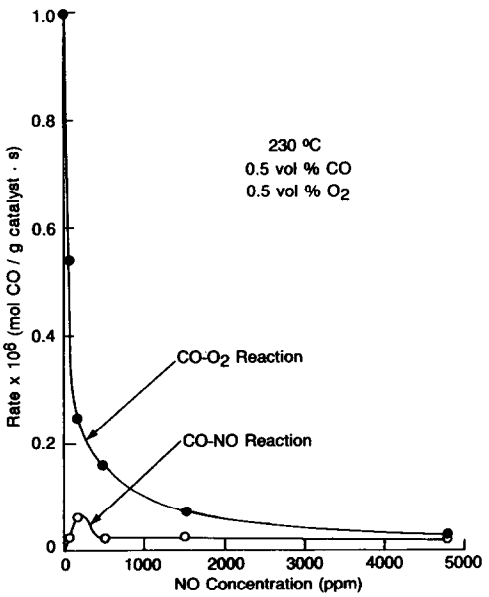

FIG. 3. Rates of the CO–O_2 and CO–NO reactions over Rh/Al_2O_3 as a function of NO concentration. Temperature and CO and O_2 concentrations were held constant.

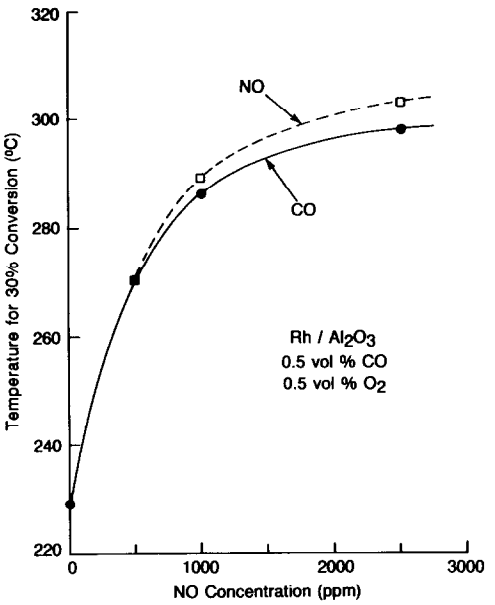

FIG. 4. Temperatures for 30% conversion of CO and NO over Rh/Al_2O_3 in a feedstream containing 0.5 vol% CO, 0.5 vol% O_2, and variable levels of NO.

that the rate of the CO–O_2 reaction is retarded markedly even in the presence of relatively small amounts of NO in the reaction mixture. In the NO concentration regime likely to be encountered in automobile exhaust (>500 ppm), however, the CO–O_2 reaction rate decreases gradually with increasing NO concentration, approaching the rate of the CO–NO reaction. This observation of similar rates for the CO–O_2 and CO–NO reactions in the CO–NO–O_2 mixture at the high NO concentration limit is consistent with the results of Fig. 2.

The impact of the NO inhibition effect discussed above on catalyst lightoff temperature was assessed by conducting temperature run-up experiments in laboratory feedstreams containing 0.5 vol% CO, 0.5 vol% O_2, and variable levels of NO. The experiments were done at a space velocity of 31,000 h^{-1} (2.5 liters/min through 2.3 g of catalyst) typical of automobile catalytic converter operation. The results of such experiments are shown in Fig. 4. The temperature required for 30% CO conversion (a measure of the extent of the overall reac-

tion) increased from 229 to 297°C as the NO concentration in the feedstream increased from 0 to 2500 ppm. In accord with the results of Fig. 3, the catalyst lightoff temperature is more sensitive to NO concentration variations in the low NO concentration regime than it is in the high concentration regime. Also included in Fig. 4 is the curve for 30% NO conversion temperatures (a measure of the extent of the CO–NO reaction). The close similarity between the two 30% conversion curves over the NO concentration range of 500 to 2500 ppm indicates that the NO in the feedstream was converted at roughly the same temperature as the CO, despite the drastic difference in the inherent rates of the $CO–O_2$ and CO–NO reactions themselves (see Fig. 2).

Despite the strong inhibition of the rate of the $CO–O_2$ reaction by NO, the $CO–O_2$ reaction kinetics in $CO–NO–O_2$ mixtures are characterized by reaction orders in CO and O_2 similar to those for the $CO–O_2$ reaction in the absence of NO. Figure 5 shows the rate of the $CO–O_2$ reaction as a function of CO concentration in the presence of 500 ppm NO (O_2 concentration fixed at 0.5 vol%). As was previously observed for the

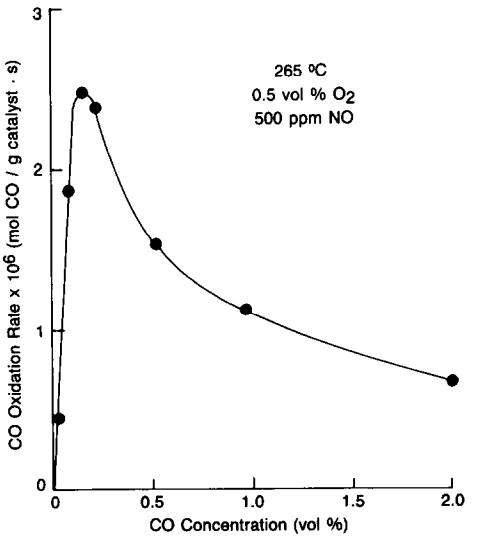

FIG. 5. Effect of CO concentration on the rate of the $CO–O_2$ reaction over Rh/Al_2O_3 at 265°C. The concentrations of O_2 and NO were held constant.

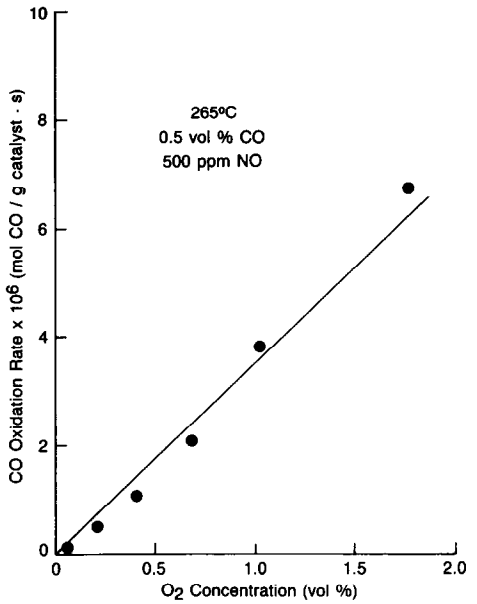

FIG. 6. Effect of O_2 concentration on the rate of the $CO–O_2$ reaction over Rh/Al_2O_3 at 265°C. The concentrations of CO and NO were held constant.

$CO–O_2$ reaction itself over the same Rh/Al_2O_3 catalyst (*7*), the rate data for CO oxidation in the presence of NO exhibits a transition from the positive-order regime (low CO concentrations) to the negative-order regime (high CO concentrations). Furthermore, additional rate measurements as a function of oxygen concentration in the presence of 500 ppm NO (see Fig. 6) show that the rate of the $CO–O_2$ reaction in $CO–NO–O_2$ mixtures increases linearly with increasing O_2 concentration. This is again in agreement with results previously reported for the $CO–O_2$ reaction in the absence of NO (*7*).

It is interesting to examine how the kinetic behavior of Pt/Al_2O_3 in $CO–NO–O_2$ mixtures compares with the observations we have described thus far for Rh/Al_2O_3. We pursued this aspect by conducting temperature run-up experiments with the 0.05 wt% Pt/Al_2O_3 catalyst under the same operating conditions (0.5 vol% CO, 0.5 vol% O_2, variable NO; 31,000 h^{-1}) that were used in Fig. 4. The results are shown in Fig. 7, where the temperature for 30% CO conversion is plotted as a function of NO concen-

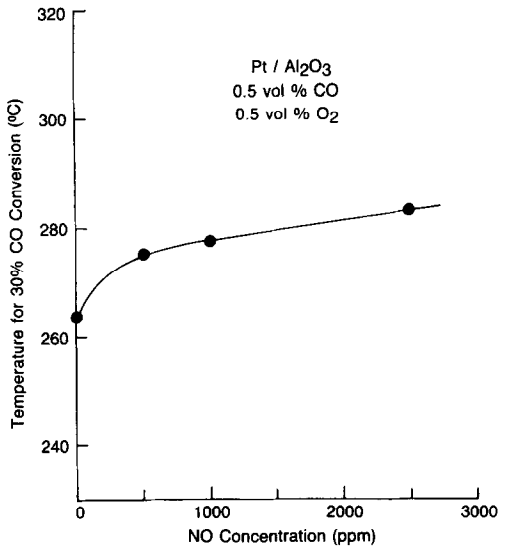

FIG. 7. Temperature for 30% CO conversion over Pt/Al_2O_3 in a feedstream containing 0.5 vol% CO, 0.5 vol% O_2, and variable levels of NO.

tration in the feed. (Only a small amount of NO was converted over the Pt/Al_2O_3 catalyst at the experimental conditions of Fig. 7.) It is evident from comparison of Figs. 4 and 7 that CO oxidation activity of the Pt/Al_2O_3 catalyst is much less affected by NO; its 30% CO conversion temperature increased only by 20°C (compared to ~70°C increase for Rh/Al_2O_3) as the feedstream concentration of NO increased from 0 to 2500 ppm.

DISCUSSION

Our results certainly attest to the strong inhibition by NO of the CO oxidation rate over the Rh/Al_2O_3 catalyst in CO–NO–O_2 mixtures. Although the presence of NO in the feedstream can lead to the formation of isocyanate species (NCO) over alumina-supported noble metal catalysts (*15–17*), we believe that these species are not responsible for the NO inhibition effect observed in this study for the following reasons. First, under the net-oxidizing conditions of Figs. 3 and 4, the amount of NCO species on the surface is expected to be small (*18*). In fact, additional activity measurements under more strongly oxidizing conditions (where the surface coverage of NCO would be even smaller) still showed a similar NO inhibition effect on CO oxidation, as shown in Fig. 8. It should be noted that oxide formation on the Rh surface is not expected to be a factor in Fig. 8; a previous surface study of Rh field emitters during CO oxidation at a comparable temperature (500 K) detected no significant Rh oxide formation until the O_2/CO concentration ratio in the gas phase reached 40 (*19*). Our argument for a lack of significant contribution by NCO species to the observed activity suppression is further supported by the results of a recent infrared study by Hecker and Bell (*20*), which suggest that the isocyanate species formed on the Rh surface readily migrates onto the support and thus is not directly involved in the catalysis.

It is important to emphasize that the NO inhibition of CO oxidation activity does not reflect an irreversible change in the catalyst itself; a plot of CO conversion efficiency vs NO concentration in Fig. 8 yielded essen-

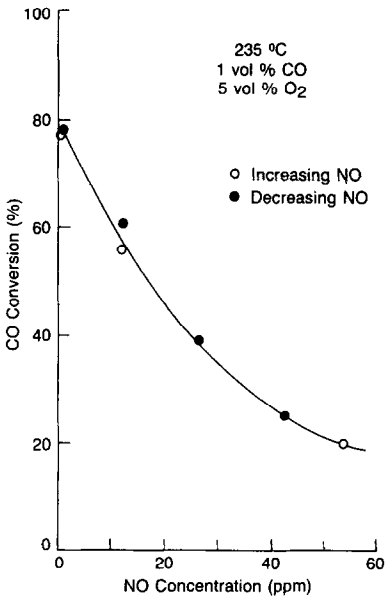

FIG. 8. Changes in CO conversion over Rh/Al_2O_3 with NO concentration in a strongly oxidizing feedstream. The feedstream concentrations of CO and O_2 were held constant.

tially the same curve regardless of the direction of NO concentration change. In view of such reversibility of the NO inhibition effect and the observation of no significant changes in the reaction orders for CO oxidation in CO–NO–O_2 mixtures (see Figs. 5 and 6), we propose that the observed activity suppression is due to blocking of the Rh sites by molecularly adsorbed NO rather than to changes in the reaction mechanism in the presence of NO. This proposed interpretation is consistent with previous infrared spectroscopic studies (*9, 21, 22*), which indicate that molecularly adsorbed NO (rather than CO) is the dominant species present on supported Rh surfaces during the reduction of NO by CO. (This observation is expected to carry over to the case of the CO–NO–O_2 system because the surface coverage by oxygen would be very low as a result of its low sticking coefficient.) The adsorbed NO molecules remain largely unreactive until they are dissociated into adsorbed nitrogen and oxygen atoms (*7, 9*). This NO dissociation process is believed to be the rate-limiting step for the CO–NO reaction over supported Rh catalysts (*7, 9, 23*). The occurrence of significant NO dissociation (as encountered during the onset of the CO–NO reaction) would lead to increased availability of sites for the CO–O_2 reaction because the resulting adsorbed N and O atoms are readily removed from the catalyst surface as a result of subsequent surface reactions (*7, 9, 24*). In this case, then, the onset of *both* the CO–O_2 and CO–NO reactions in CO–NO–O_2 mixtures would be expected to be controlled by the dissociation of chemisorbed NO, resulting in the near simultaneity of the lightoff of these two reactions as observed in Fig. 2.

The observations made in Figs. 2 and 4 clearly demonstrate the importance of the CO–NO reaction in determining the kinetic behavior of the CO–NO–O_2 reaction system over supported Rh; that is, no significant reaction occurs until conditions become favorable for the CO–NO reaction. Thus, useful insight into the behavior of the CO–NO–O_2 system can be gained by focusing on the CO–NO reaction system itself. As discussed above, the key factor controlling the reaction rates appears to be the surface population of molecularly adsorbed NO and its dissociation rate. In addition to *in situ* infrared spectroscopy, kinetic experiments are often useful in identifying major surface species present under reaction conditions. The rate of the CO–NO reaction over the 0.01 wt% Rh/Al_2O_3 catalyst exhibits a negative-order dependence on the gas-phase concentration of NO at NO concentrations of practical interest (see Fig. 9). This is in agreement with previous infrared observations (*9, 21, 22*) that supported Rh surfaces are predominantly covered with adsorbed NO molecules during the CO–NO reaction. Similar rate measurements at 450°C over the 0.05 wt% Pt/Al_2O_3 catalyst, on the other hand, show a positive-order dependence on NO concentration (see Fig. 10), indicating that the coverage of the Pt surface by chemisorbed NO is relatively small during the CO–NO reaction. The rate data of Fig. 10 also display the inhibition

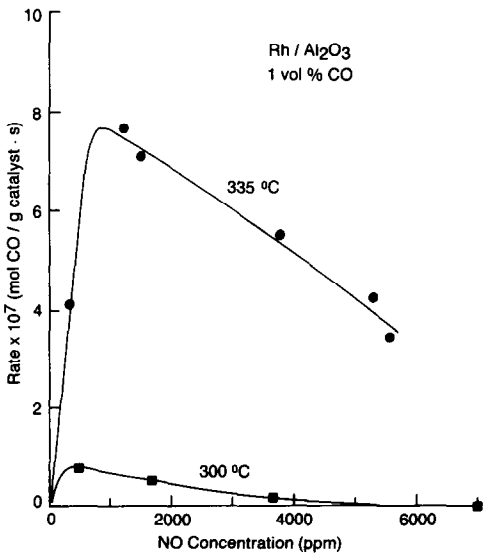

FIG. 9. Rate of CO–NO reaction (in the absence of O_2) over Rh/Al_2O_3 as a function of NO concentration at two different temperatures.

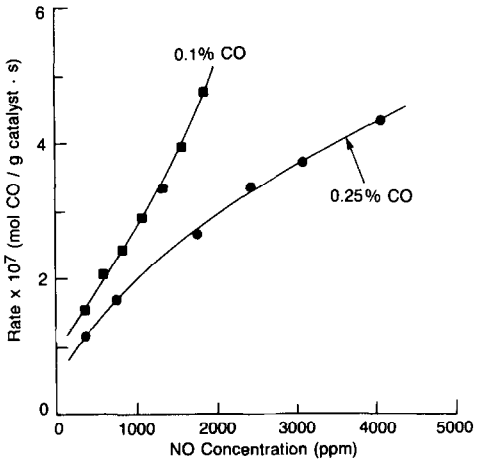

FIG. 10. Rate of the CO–NO reaction (in the absence of O_2) over Pt/Al_2O_3 as a function of NO concentration at two different CO concentration levels.

effect of CO on the reaction rate. Thus, in accordance with previous infrared studies (*10, 25*), our rate measurements indicate the the Pt surface adsorbs CO much more strongly than NO under reaction conditions. The resulting low surface coverage by NO on the Pt surface (as opposed to high NO coverages on Rh) explains why the magnitude of the NO inhibition effect on CO oxidation rate is substantially smaller over the Pt/Al_2O_3 catalyst than that over the Rh/Al_2O_3 catalyst (compare Figs. 4 and 7).

We made cursory examinations of the following two questions pertinent to the NO inhibition effect on the CO oxidation rate over Rh/Al_2O_3. First, does the NO inhibition effect observed for simple CO–NO–O_2 feedstreams carry over to more complex exhaust-like feedstreams? Second, how does the magnitude of the rate inhibition by NO compare with that by SO_2 (which is also known to cause largely reversible deactivation of noble metal catalysts)? In order to address these questions, we conducted temperature run-up experiments with the 0.01 wt% Rh/Al_2O_3 catalyst using an integral reactor made of quartz. The reactor was electrically heated at a rate of approximately 10°C/min and the feedstream included 0.77 vol% CO, 300 ppm propylene, 1 vol% O_2, 0.2 vol% H_2, 10 vol% H_2O, 10 vol% CO_2, 0 or 500 ppm NO, and 0 or 20 ppm SO_2 in a N_2 background. The results of the experiments are displayed in Table 1 in a two-dimensional framework. It is clear from Table 1 that the strong NO inhibition effect on the CO oxidation over Rh/Al_2O_3 (nearly 50°C delay in catalyst lightoff) still prevails in the synthetic exhaust gas stream regardless of whether SO_2 is present in the feed or not. Also, the presence of 20 ppm SO_2, a typical level in automobile exhaust, was found to have a rather small detrimental effect on the CO oxidation activity of the Rh/Al_2O_3 catalyst, causing only 5–10°C increases in the 50% CO conversion temperature.

CONCLUDING REMARKS

The presence of NO in the reactant stream prevents the occurrence of the CO–O_2 reaction over Rh/Al_2O_3 until the extent of the CO–NO reaction becomes significant, presumably due to site blocking by molecularly adsorbed NO. As a result of this NO inhibition effect on the CO oxidation rate, the onset of both the CO–O_2 and CO–NO reactions in CO–NO–O_2 mixtures occurs simultaneously near the lightoff temperature for the CO–NO reaction system itself. This kinetic interaction among the reactant species invalidates the use of simple CO oxidation kinetics (i.e., those obtained in the absence of NO) to predict CO removal from engine exhaust. This observation also implies that the overall kinetic behavior of Rh/Al_2O_3 in CO–NO–O_2 mixtures is dominated by the features char-

TABLE 1

50% CO Conversion Temperatures in Synthetic Exhaust[a]

	No SO_2	20 ppm SO_2
No NO	235°C	241°C
500 ppm NO	281°C	290°C

[a] Rh/Al_2O_3 (0.01 wt%); the feed always contained CO, HC, O_2, H_2, H_2O, and CO_2 in a N_2 background.

acteristic of the CO–NO reaction (rather than the CO–O_2 reaction), thus demonstrating the importance of understanding the CO–NO reaction in the development of improved automotive Rh catalysts.

The magnitude of the NO inhibition effect on the CO oxidation over Pt/Al_2O_3 is considerably smaller than that over Rh/Al_2O_3. This is reasonable in view of the different adsorption characteristics of CO and NO on the two surfaces; that is, NO is the dominant species present on the Rh surface while the Pt surface is predominantly covered with CO (i.e., relatively low NO coverages). This difference in the adsorption characteristics between Pt and Rh surfaces makes Pt/Rh bimetallic catalysts (such as commercial automotive catalysts) a particularly interesting example for further study.

REFERENCES

1. Taylor, K. C., *in* "Catalysis: Science and Technology" (J. R. Anderson and M. Boudart, Eds.), Vol. 5, p. 119. Springer-Verlag, Berlin, 1984.
2. Kummer, J. T., *Prog. Energy Combust. Sci.* **6,** 177 (1980).
3. Hegedus, L. L., and Gumbleton, J. J., *Chem. Tech. (Leipzig)* **10,** 630 (1980).
4. Wei, J., "Advances in Catalysis," Vol. 24, p. 57. Academic Press, New York, 1975.
5. Engel, T., and Ertl, G., "Advances in Catalysis," Vol. 28, p. 1. Academic Press, New York, 1979.
6. Campbell, C. T., Shi, S.-K., and White, J. M., *Appl. Surf. Sci.* **2,** 382 (1979).
7. Oh, S. H., Fisher, G. B., Carpenter, J. E., and Goodman, D. W., *J. Catal.* **100,** 360 (1986).
8. Root, T. W., Schmidt, L. D., and Fisher, G. B., *Surf. Sci.* **150,** 173 (1985).
9. Hecker, W. C., and Bell, A. T., *J. Catal.* **84,** 200 (1983).
10. Lorimer, D., and Bell, A. T., *J. Catal.* **59,** 223 (1979).
11. Voltz, S. E., Morgan, C. R., Liederman, D., and Jacob, S. M., *Ind. Eng. Chem. Prod. Res. Dev.* **12,** 294 (1973).
12. Oh, S. H., and Carpenter, J. E., *J. Catal.* **80,** 472 (1983).
13. Berty, J. M., *Chem. Eng. Prog.* **70,** 78 (1974).
14. D'Aniello, M. J., Jr., "Method of Marking Layered Catalysts," U.S. Patent No. 4,380,510, April 19, 1983.
15. Unland, M. L., *Science* **179,** 567 (1973).
16. Unland, M. L., *J. Phys. Chem.* **77,** 1952 (1973).
17. Unland, M. L., *J. Catal.* **31,** 459 (1973).
18. Chang, C. C., and Hegedus, L. L., *J. Catal.* **57,** 361 (1979).
19. Kellogg, G. L., *J. Catal.* **92,** 167 (1985).
20. Hecker, W. C., and Bell, A. T., *J. Catal.* **85,** 389 (1984).
21. Arai, H., and Tominaga, H., *J. Catal.* **43,** 131 (1976).
22. Solymosi, F., and Sarkany, J., *Appl. Surf. Sci.* **3,** 68 (1979).
23. Chin, A. A., and Bell, A. T., *J. Phys. Chem.* **87,** 3700 (1983).
24. Campbell, C. T., and White, J. M., *Appl. Surf. Sci.* **1,** 347 (1978).
25. Brown, M. F., and Gonzalez, R. D., *J. Catal.* **44,** 477 (1976).